Available online at www.sciencedirect.com
ScienceDirect
Estuarine, Coastal and Shelf Science 70 (2006) 423–437
ESTUARINE COASTAL AND SHELF SCIENCE
www.elsevier.com/locate/ecss

Dissolved oxygen stratification in two micro-tidal partially-mixed estuaries

Jing Lin [a,*], Lian Xie [a], Len J. Pietrafesa [b], Jian Shen [c], Michael A. Mallin [d], Michael J. Durako [d]

[a] Department of Marine, Earth, and Atmospheric Sciences, North Carolina State University, Raleigh, NC 27695, United States
[b] College of Physical & Mathematical Sciences, North Carolina State University, Raleigh, NC 27695, United States
[c] Virginia Institute of Marine Science, School of Marine Science, The College of William and Mary, Gloucester Point, VA 23062, United States
[d] Center for Marine Science, University of North Carolina Wilmington, Wilmington, NC 28409, United States

Received 7 November 2005; accepted 13 June 2006
Available online 21 August 2006

Abstract

The controlling physical factors for vertical oxygen stratification in micro-tidal, partially-mixed estuaries are discussed in this paper. A theoretical deduction shows that vertical stratification of dissolved oxygen (DO) concentration can be explained by the extended Hansen and Rattray's Central Region theory, which suggests that in addition to biological factors such as photosynthesis, biochemical oxygen demand (BOD), sediment oxygen demand (SOD), vertical DO profiles are mainly controlled by physical factors such as surface re-aeration, river flow, and estuarine gravitational circulation. Vertical mixing of DO from surface re-aeration and photosynthesis sets a DO profile of higher concentration near the surface and lower near the bottom. With a positive seaward longitudinal DO gradient, strong river flow and estuarine gravitational circulation can cause lower DO concentrations near the surface and higher near the bottom. The actual vertical oxygen profile is then determined by the relative magnitude of the above-mentioned mechanisms. It is sensitive to two parameters: (1) the strength of the gravitational circulation (u_E); and (2) the relative importance between biochemical oxygen demand and vertical diffusivity (α).

Vertical DO stratification usually becomes weaker as u_E increases. The impact of gravitational circulation on vertical oxygen distribution becomes more important for a larger α. The impact of α on oxygen stratification is profound. As u_E (and river flow) increases, DO stratification appears to be less sensitive to the value of α. Surface-to-bottom differences in DO concentrations (ΔDO) is negligible when α is small ($\alpha < 0.5$). As α increases, ΔDO increases under a weak to moderate gravitational circulation mode ($u_E \leq 5$ cm s^{-1}). Under a strong gravitational circulation mode, ΔDO becomes negative with a small α ($\alpha < 2$), and as α continues to increase, ΔDO becomes positive.

The newly-deduced governing equation for vertical oxygen stratification is applied to two micro-tidal, partially-mixed estuarine systems: the Cape Fear River Estuary (CFRE) and the Pamlico River Estuary (PRE) of North Carolina. In the CFRE, although strong vertical salinity stratification exists, DO concentrations are usually well mixed. De-coupling between salinity stratification and oxygen stratification is mainly due to a relatively stronger estuarine gravitational circulation and higher freshwater inflow in the system. It appears that river flow and gravitational circulation are the dominant factors in controlling oxygen stratification in the CFRE.

In contrast, vertical stratification of DO concentrations is closely correlated with that of salinity in the PRE. In the PRE, the estuarine gravitational mode and river flow are often both very weak, and DO stratification is very sensitive to the value of α. With negligible influence from tidal mixing, the system is more sensitive to vertical mixing regulated by salinity stratification and wind. As a result, vertical DO stratification is closely correlated with salinity stratification in the PRE.

Keywords: dissolved oxygen; stratification; estuarine gravitational circulation; vertical mixing; Cape Fear River; Pamlico River

* Corresponding author. Department of Marine, Earth, and Atmospheric Sciences, North Carolina State University, Campus Box 8208, Raleigh, NC 27695, United States.
E-mail address: jlin3@ncsu.edu (J. Lin).

0272-7714/$ - see front matter © 2006 Elsevier Ltd. All rights reserved.
doi:10.1016/j.ecss.2006.06.032

1. Introduction

Coastal environments have undergone profound changes over the past 50 years. Population growth and accompanying land-use changes have resulted in a number of significant problems in coastal regions. These problems include eutrophication, harmful algal blooms, modification and loss of habitat, chemical contamination and hypoxia/anoxia (Cloern, 2001; Boesch, 2002; Howarth et al., 2003).

Low/no dissolved oxygen (hypoxia/anoxia), a direct consequence of nutrient over-enrichment, is one of the most prominent stressors of estuarine and coastal aquatic biota. Hypoxia is closely associated with declined shell fish productions and massive fish kills in many systems (Pietrafesa and Miller, 1997; Nestlerode and Diaz, 1998). Hypoxia and anoxia degrade bottom habitats through a wide suite of mechanisms. Under conditions of limited oxygen at the bottom, rates of nitrogen and phosphorous remineralization and sulfate reduction increase (Diaz and Rosenberg, 1995; Holmer, 1999). The resulting production of sulfide in combination with low oxygen can prove lethal to benthic organisms (Diaz and Rosenberg, 1995; Holmer, 1999). Because benthic macrofauna serve as essential prey resources for demersal fishes, sustained hypoxia can have significant trophic implications (Nestlerode and Diaz, 1998; Peterson et al., 2000; Tankersley and Wieber, 2000; Taylor and Eggleston, 2000; Eby and Crowder, 2002, 2004).

In recent years, hypoxic conditions have been reported in estuaries and coastal seas globally (Kuo et al., 1991; Stanley and Nixon, 1992; Buzzelli et al., 2002; Kurup and Hamilton, 2002; Diaz et al., 2004; Glenn et al., 2004; Hagy et al., 2004; Ishikawa et al., 2004; Scavia et al., 2004; Yin et al., 2004). In addition to biological factors such as excess nutrient and organic matter loads from their drainage basins, in situ phytoplankton blooms, excess nitrification, and strong sediment oxygen demand, physical factors such as water temperature, vertical stratification, and estuarine circulation have also been observed as controlling factors in vertical distributions of dissolved oxygen (DO) and the evolution of bottom hypoxia.

Stanley and Nixon (1992) examined the relationships among bottom DO, vertical stratification, and factors responsible for stratification–destratification in the Pamlico River Estuary (PRE), and found that hypoxia develops only when vertical stratification and warm water temperature occur concurrently. Stratification inhibits oxygen fluxes from the surface waters through reduced vertical mixing. Warm temperature not only reduces oxygen saturation in the water column, but also enhances biochemical oxygen demand (BOD) and sediment oxygen demand (SOD). The close correlation between vertical stratification, warm temperature and bottom-water hypoxia was also identified in many other estuaries including the Neuse River, USA (Borsuk et al., 2001; Buzzelli et al., 2002), Swan River, Australia (Kurup and Hamilton, 2002), Patuxent River, USA (Breitburg et al., 2003), and Narragansett Bay, USA (Bergondo et al., 2005).

Similarly, Kuo and Neilson (1987) found that when water temperature exceeded 20 °C, low oxygen concentrations (<50% saturation) were observed in the majority (>50%) of the surveys in the Rappahannock and York Rivers in Virginia. In contrast, although the James River Estuary received a relatively larger amount of nutrients and organic matter, low oxygen concentration was rarely observed (about 2% of the surveys). Through an oxygen budget analysis, they concluded that the rare occurrence of bottom hypoxia in the James River is due to the stronger net movement of the bottom waters. The role of estuarine circulation in affecting bottom DO distributions was also observed in other estuaries worldwide (Ishikawa et al., 2004; Yin et al., 2004).

It appears that vertical distributions of DO concentrations in estuaries are affected by different physical parameters in different systems. The dominant physical parameters in a system are often unknown a priori. To predict DO variations in estuaries, two types of models are usually applied. The first type is simple probabilistic models, which are mainly based on statistical relationships between DO concentrations and environmental data collected in the estuary concerned. For example, a generalized additive (statistical) model was used to explore the major relationships between bottom-water oxygen concentration, vertical stratification, and temperature in the Neuse River Estuary (Borsuk et al., 2001). Kauppila et al. (2003) developed a statistical model to predict oxygen concentration and percentage saturation based on water chemistry, estuary morphometry, and land-use characteristics for 19 estuaries in the northern Baltic Sea. The second type of oxygen prediction models is process-based, dynamic simulation models. Research on oxygen in estuaries and coastal waters has generally taken this approach. This type of models usually starts with a mass conservation equation, where both oxygen sources and sinks are explicitly expressed. For example, in addition to the statistical model, Borsuk et al. (2001) developed a simple process-based box model to predict bottom oxygen concentrations in the Neuse River. The processes considered are vertical mixing and sediment/biological oxygen demand. A laterally-integrated, two-dimensional, real-time model (HEM-2D) was applied in the Tidal Rappahannock River to study the effects of physical processes (gravitational circulation and vertical mixing), oxygen demand, and the quality of incoming bay water on bottom hypoxia (Park et al., 1996). Lung and Bai (2003) developed a water quality model for the Patuxent Estuary using the modeling framework CE-QUAL-W2 to address the impact of current and projected land-use changes on the water quality (including chlorophyll *a*, nutrients, and dissolved oxygen concentrations). Ishikawa et al. (2004) used a laterally-integrated, two-dimensional model to explore the onset and evolution of bottom hypoxia in the Tone River. Some complex, spatially and temporally detailed representation, three-dimensional water quality models were also used in many of the estuaries and coastal bays (Cerco and Cole, 1993; Wool et al., 2003; Zheng et al., 2004).

This study aims to examine the dominant physical factors in controlling vertical DO distributions in estuarine waters. In particular, the study focuses on two micro-tidal, partially-mixed estuaries: the Pamlico and Cape Fear River Estuaries (Fig. 1). Biological processes such as variations of nutrient

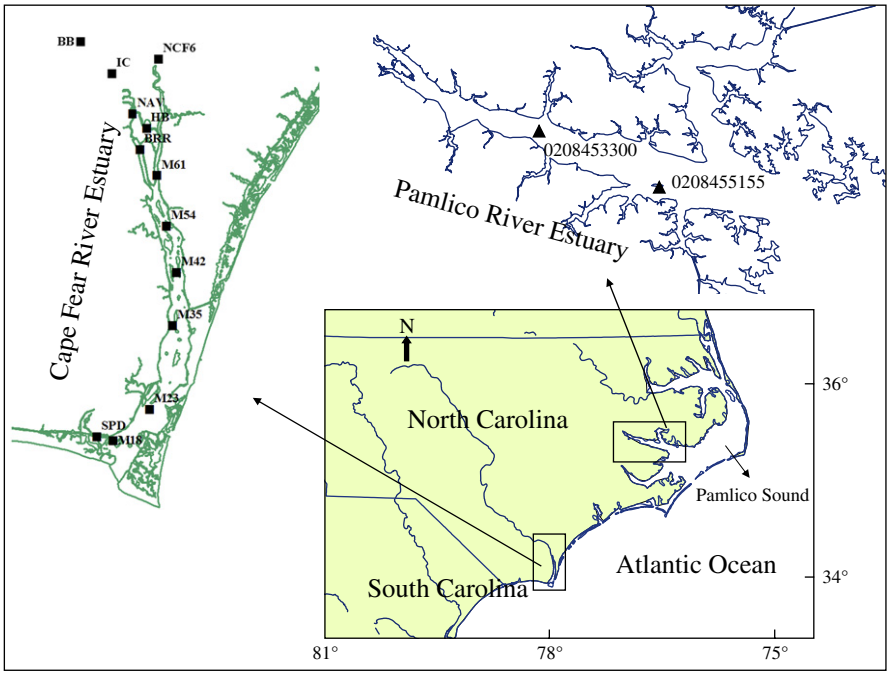

Fig. 1. The study area. The squares indicate monitoring stations in the Cape Fear River Estuary and the triangles indicate monitoring stations in the Pamlico River Estuary.

and organic matter loads, in situ phytoplankton blooms, and strong sediment oxygen demand are considered here with their most simplified forms. Since hypoxia normally occurs during summer seasons with warm temperatures, biological functions considered here are all assumed to be associated with temperature around or above 20 °C.

2. Theoretical considerations

Because prolonged hypoxic conditions can have significant impacts on benthic organisms and thus have trophic implications (Nestlerode and Diaz, 1998; Peterson et al., 2000), in the following theoretical development of oxygen stratification, tidally-averaged dependent variables are considered. We assume the estuary is rectangular in cross-section, with constant cross-sectional area and depth. The along-channel, tidally-averaged velocity $u(x, z)$ and salinity $s(x, z)$ can be split into depth-averaged and depth-varying parts:

$$u = \overline{u}(x) + u'(x,z), \quad s = \overline{s}(x) + s'(x,z) \tag{1}$$

where $\overline{u}$ and $\overline{s}$ are depth-averaged parts and u' and s' are depth-varying parts. The along-channel momentum balance may be approximated by (Dyer, 1997):

$$0 = -\frac{1}{\rho_0}p_x + (K_M u_z)_z \tag{2}$$

where a subscript of x or z indicates a partial derivative in longitudinal and vertical directions, respectively, ρ_0 is the water density, p_x is the longitudinal pressure gradient, and K_M is the vertical eddy viscosity. Assuming that the pressure is hydrostatic, and that the longitudinal or major axial gradient of the depth-varying salinity is much smaller than the longitudinal gradient of the depth-averaged salinity, i.e. $s'_x \ll \overline{s}_x$ (Pritchard, 1952), the pressure gradient can be written as:

$$-\frac{1}{\rho_0}p_x = -g\eta_x + g\beta\overline{s}_x z \tag{3}$$

where $g = 9.8\ \mathrm{m\,s^{-2}}$ is the gravitational acceleration constant, η is the tidally-averaged surface elevation, and the salinity-affected water density is approximated as $\rho = \rho_0(1 + \beta s)$, where $\beta \approx 7.7 \times 10^{-4}\ \mathrm{ppt^{-1}}$. Eqs. (2) and (3) can be combined to give:

$$(K_M u_z)_z = g\eta_x - g\beta\overline{s}_x z \tag{4}$$

For a vertically uniform K_M, Eq. (4) leads to (MacCready, 2004):

$$u_{zzz} = -\frac{g\beta\overline{s}_x}{K_M} \tag{5}$$

The boundary conditions are no-slip on the bottom, $u(z = -H) = 0$; a rigid lid, $u_z(z = 0) = 0$; and the net flow through a cross-section is equal to the river input or $H^{-1}\int_{-H}^{0} u\,\mathrm{d}z \equiv \overline{u} = Q_R/A$, where Q_R is the river discharge and A is the cross-sectional area. Integrating Eq. (5) (Hansen and Rattray, 1965; Officer, 1976; MacCready, 2004) yields:

$$u' = \overline{u}P_1 + u_E P_2 \tag{6}$$

$$P_1 = \frac{1}{2} - \frac{3}{2}\xi^2, \quad P_2 = 1 - 9\xi^2 - 8\xi^3$$

where $\xi = z/H$ and $u_E = g\beta\overline{s}_x H^3/(48K_M)$. The vertical profile of tidally-averaged velocity is determined by two terms: the river flow ($\overline{u}P_1$), and the estuarine gravitational circulation ($u_E P_2$).

The salt conservation equation can be written as:

$$s_t + \frac{1}{A}(usA)_x + (ws)_z = \frac{1}{A}(K_H s_x A)_x + (K_S s_z)_z \tag{7}$$

where w is the vertical velocity, K_H is the horizontal diffusivity and K_S is the vertical diffusivity. The vertically-averaged salt balance equation can be expressed as:

$$\overline{s}_t + \frac{1}{A}(\overline{u}\,\overline{s}A) + \frac{1}{A}(\overline{u's'}A)_x = \frac{1}{A}(K_H\overline{s}_x A)_x \tag{8}$$

Subtracting Eq. (8) from Eq. (7) and assuming $s'_x \ll \overline{s}_x$, the dominant steady-state balance for s' can be written as (Pritchard, 1954):

$$u'\overline{s}_x \cong K_S s'_{zz} \tag{9}$$

Integrate Eq. (9) with the zero flux boundary conditions (i.e., the vertical salt flux vanishes at the surface and the bottom boundaries), the vertical salinity profile is solved as follows (Hansen and Rattray, 1965; Officer, 1976; MacCready, 2004):

$$s' = \frac{H^2}{K_S}\overline{s}_x(\overline{u}P_3 + u_E P_4) \tag{10}$$

$$P_3 = -\frac{7}{120} + \frac{1}{4}\xi^2 - \frac{1}{8}\xi^4 \tag{11}$$

$$P_4 = -\frac{1}{12} + \frac{1}{2}\xi^2 - \frac{3}{4}\xi^4 - \frac{2}{5}\xi^5 \tag{12}$$

This shows that the vertical salinity profile depends on the mean flow due to river discharge (the first term of Eq. (10)) and the estuarine gravitational circulation (the second term of Eq. (10)).

In addition to the physical processes controlling salinity distributions (i.e. the mean flow due to river discharge and the estuarine gravitational circulation) in estuaries, dissolved oxygen (designated as O in the following theoretical developments) dynamics are influenced by other physical and biological factors as extra sources and sinks. Surface re-aeration from the atmosphere and photosynthetic oxygen production are the major DO sources. Aquatic respiration (the "breathing" of all living organisms in the water), DO consumption by chemical oxygen demand (COD) and SOD are all DO sinks (Thomann and Mueller, 1987). Surface re-aeration is mainly through vertical diffusion processes at the air–water interface, and hence the corresponding function is included in the DO mass balance equation through enforcing a flux boundary condition at the surface boundary. SOD will be applied as the bottom boundary condition. DO consumption by COD is usually expressed as a first-order decay function (Thomann and Mueller, 1987; Chapra, 1997; Borsuk et al., 2001). The mass balance equation for dissolved oxygen is expressed as:

$$O_t + \frac{1}{A}(uOA)_x + (wO)_z = \frac{1}{A}(K_H O_x A)_x + (K_S O_z)_z + P - R - K_{COD}\mathrm{COD} \tag{13A}$$

where P is the oxygen production rate through photosynthesis, R is the DO consumption rate through biomass respiration, and K_{COD} is the COD decay rate. Assuming COD is a constant in the water column, and both R and K_{COD} are proportional to DO concentrations (Thomann and Mueller, 1987; Chapra, 1997), combining DO consumption from both COD decay and biomass respiration, we have:

$$O_t + \frac{1}{A}(uOA)_x + (wO)_z = \frac{1}{A}(K_H O_x A)_x + (K_S O_z)_z + P - \gamma O \tag{13B}$$

where γ is a function of both COD and biomass. For simplicity, γ is assumed to be a constant. Applying boundary conditions of $K_S O_z(z=0) = \theta_S$ and $K_S O_z(z=-H) = \theta_B$, where θ_S is the surface oxygen flux and θ_B is the bottom oxygen flux, the depth-averaged dissolved oxygen ($\overline{O}$) mass balance equation is expressed as:

$$\overline{O}_t + \frac{1}{A}(\overline{u}\overline{O}A)_x + \frac{1}{A}(\overline{u'O'}A)_x = \frac{1}{A}(K_H\overline{O}_x A)_x + \overline{P} - \gamma\overline{O} + \frac{1}{H}(\theta_S - \theta_B) \tag{14}$$

Subtracting Eq. (14) from Eq. (13B) and assuming $O'_x \ll \overline{O}_x$, the dominant steady-state balance for O' can be written as:

$$u'\overline{O}_x \cong K_S O'_{zz} + P' - \gamma O' - \frac{1}{H}(\theta_S - \theta_B) \tag{15}$$

Using $\xi = z/H$ to replace z and Eq. (6) to represent u', Eq. (15) gives:

$$O'_{\xi\xi} - \alpha^2 O' = \frac{H^2}{K_S}\overline{O}_x(\overline{u}P_1 + u_E P_2) - \frac{H^2}{K_S}P' + \frac{H}{K_S}(\theta_S - \theta_B) \tag{16}$$

where

$$\alpha^2 = \left(\frac{H^2}{K_S}\right)\gamma = \frac{\text{time scale for vertical diffusion}}{\text{time scale for BOD decay}}$$

which is a constant parameter indicating the relative importance between BOD decay and vertical diffusion. The vertical diffusivity, K_S, is usually on the order of $10^{-4}\,\mathrm{m^2\,s^{-1}}$ in estuaries (Hetland and Geyer, 2004), O(H) (the order of magnitude of H) is usually around 10 m. O(γ) is around $10^{-6}\,\mathrm{s^{-1}}$ (Borsuk et al., 2001). As a result, O(α) ≈ 1.

The photosynthetic oxygen production rate, P, is usually greater in the surface waters where light intensity is high (Kirk, 1994). To account for different depth-varying profiles of P, three types of functions are used: (1) P is assumed to be uniformly distributed in the water column and hence $P' = 0$; (2) P is maximized at the surface with a value of P_M, and decreases exponentially downward, $P = P_M e^{k\xi}$, where k is a constant and the depth-varying part becomes

$P' = P_M\big((ke^{k\xi} - 1 + e^{-k})/k\big)$; and (3) P is maximized at the surface with a value of P_M, and decreases linearly downward, $P = P_M(1 + \lambda\xi)$, where λ is a constant and the depth-varying part becomes $P' = P_M\lambda((1/2)+\xi)$.

Integrating Eq. (16) with the three function forms of P', and applying the surface boundary condition of $O'_\xi(\xi = 0) = \theta$ and $\int_{-1}^{0} O'\,d\xi = 0$, one obtains the vertical oxygen profile as follows:

$$O' = \frac{\theta_S}{\gamma H}P_{5S} + \frac{\theta_B}{\gamma H}P_{5B} + \frac{P_M}{\gamma}P_6 + \frac{\overline{O}_x\overline{u}}{\gamma}P_7 + \frac{\overline{O}_x u_E}{\gamma}P_8 \tag{17}$$

$$P_{5S} = -\frac{1 - e^{\alpha} - \alpha^2 e^{\alpha}}{\alpha(e^{\alpha} - e^{-\alpha})}e^{\alpha\xi} - \frac{1 - e^{-\alpha} - \alpha^2 e^{-\alpha}}{\alpha(e^{\alpha} - e^{-\alpha})}e^{-\alpha\xi} - 1 \tag{18A}$$

$$P_{5B} = \frac{1 - \alpha^2 - e^{\alpha}}{\alpha(e^{\alpha} - e^{-\alpha})}e^{\alpha\xi} + \frac{1 - \alpha^2 - e^{-\alpha}}{\alpha(e^{\alpha} - e^{-\alpha})}e^{-\alpha\xi} + 1 \tag{18B}$$

$$P_6 = 0 \tag{19A}$$

$$P_6 = -\frac{\alpha^2 e^{k\xi}}{k^2 - \alpha^2} - \frac{1 - e^{-k}}{k} + \frac{k\alpha[(e^{\alpha} - e^{-k})e^{\alpha\xi} + (e^{-\alpha} - e^{-k})e^{-\alpha\xi}]}{(k^2 - \alpha^2)(e^{\alpha} - e^{-\alpha})} \tag{19B}$$

$$P_6 = \frac{\lambda}{2} + \lambda\xi + \frac{\lambda(1 - e^{\alpha})e^{\alpha\xi} + \lambda(1 - e^{-\alpha})e^{-\alpha\xi}}{\alpha(e^{\alpha} - e^{-\alpha})} \tag{19C}$$

$$P_7 = \frac{3}{2}\xi^2 - \frac{1}{2} + \frac{3}{\alpha^2} - \frac{3(e^{\alpha\xi} + e^{-\alpha\xi})}{\alpha(e^{\alpha} - e^{-\alpha})} \tag{20}$$

$$P_8 = 9\xi^2 + 8\xi^3 - 1 + \frac{18 + 48\xi}{\alpha^2} + \frac{6 + \left(\frac{48}{\alpha^2}\right)(1 - e^{\alpha})}{\alpha(e^{\alpha} - e^{-\alpha})}e^{\alpha\xi} + \frac{6 + \left(\frac{48}{\alpha^2}\right)(1 - e^{-\alpha})}{\alpha(e^{\alpha} - e^{-\alpha})}e^{-\alpha\xi} \tag{21}$$

The vertical stratification of tidally-averaged dissolved oxygen in coastal plain type, elongated (in which the axial length is much greater than the width, which is much greater than the depth) estuaries can be determined by the four terms on the right hand side of Eq. (17). They are functions of surface re-aeration and bottom oxygen demand $((\theta_S/\gamma H)P_{5S} + (\theta_B/\gamma H)P_{5B})$, photosynthesis $((P_M/\gamma)P_6)$, river flow $((\overline{O}_x\overline{u}/\gamma)P_7)$, and estuarine gravitational circulation $((\overline{O}_x u_E/\gamma)P_8)$, respectively. The three functions of P_6 correspond to the constant (Eq. (19A)), exponential (Eq. (19B)), and linear (Eq. (19C)) forms of photosynthetic oxygen production, respectively.

The sources of the dissolved oxygen in the water column include oxygen re-aeration fluxes from the atmosphere and the oxygen production from aquatic plant photosynthesis. The re-aeration oxygen flux is imported at the surface boundary of the water column and oxygen production from photosynthesis also tends to be higher in surface waters (Kirk, 1994; Chapra, 1997). The newly added oxygen is mixed toward deeper waters and at the same time is consumed by biochemical oxygen demand along its way. The vertical variation of dissolved oxygen concentrations associated with surface re-aeration is represented by function P_{5S}. In Fig. 2a, the vertical profiles of P_{5S} at different values of α show that oxygen concentrations are highest near the surface and lower in deeper waters. A higher α value (a higher BOD and/or a weaker vertical mixing in the water column) is associated with stronger oxygen stratification (defined as higher DO concentrations near the surface and lower near the bottom). In addition, oxygen fluxes due to SOD at the bottom boundary cause lower oxygen concentrations near the bed (Fig. 2b). The oxygen stratification is especially strong when α is larger. If we assume the surface oxygen fluxes are the same as the bottom oxygen fluxes, the steady-state vertical profile of DO that is caused by surface re-aeration and SOD (denoted as P_5) is shown in Fig. 2c. As α increases, the surface-to-bottom difference in P_5 (denoted as ΔP_5) increases, the rate of change in ΔP_5 is affected by the relative magnitude of bottom (θ_B) and surface (θ_S) oxygen fluxes. With the same α value and a higher SOD (or a larger value of θ_B/θ_S), oxygen stratification is stronger (ΔP_5 is larger) (Fig. 2d).

The vertical variation of dissolved oxygen concentrations associated with photosynthesis is represented by function P_6. When photosynthetic oxygen production is uniformly distributed in the water column, the vertical variation of DO concentrations caused by this function is zero (Eq. (19A)). In contrast, when photosynthetic oxygen production decreases downward exponentially or linearly, DO stratification occurs. With a more rapid decrease of photosynthetic oxygen production from the surface (larger k and λ), DO stratification becomes stronger (Fig. 3). Vertical DO profiles caused by photosynthesis functions are also affected by physical mixing. As a result, the vertical DO profiles do not follow either an exponential or a linear form. In addition, when α is small (less than 1) or, vertical mixing is strong, the differences between surface and bottom DO concentrations caused by vertical variations of photosynthetic oxygen production are negligible. DO stratification associated with depth-varying photosynthesis functions becomes significant when α is larger.

Assuming the depth-averaged oxygen concentration increases downstream, such as occurs in the Pamlico River (Stanley and Nixon, 1992), the Rappahannock River (Kuo et al., 1991), the Neuse River (Buzzelli et al., 2002), and the Cape Fear River Estuary (Mallin et al., 1999), making $\overline{O}_x$ positive, then the vertical DO stratification affected by river flow is governed by P_7 (Fig. 4). Due to the higher flow velocity near the surface (hence larger negative horizontal oxygen fluxes) and lower in the deeper waters (hence smaller negative horizontal oxygen fluxes), the DO concentration tends to be lower near the surface and higher near the bottom, which is opposite to the oxygen stratification pattern governed by P_5 and P_6.

The vertical DO variation affected by estuarine gravitational circulation is governed by P_8 (Fig. 4). With a positive $\overline{O}_x$, oxygen concentrations tend to be lower near the surface and higher near the bottom. This is due to downstream

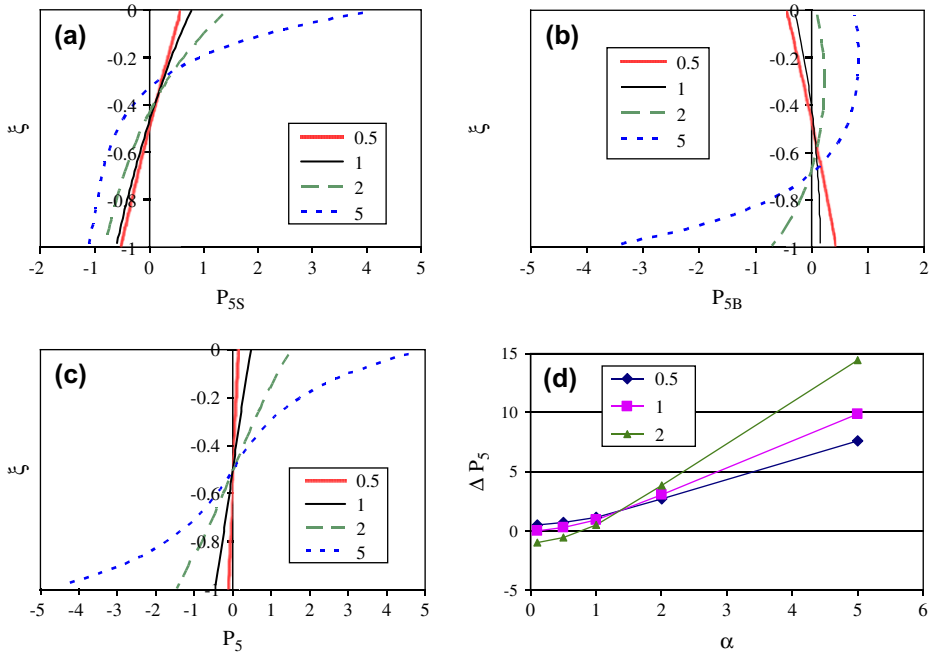

Fig. 2. Vertical distributions of (a) P_{5S}, (b) P_{5B}, and (c) $P_5 = P_{5S} + P_{5B}$ while assuming $\theta_S = \theta_B$, at different values of α (indicated by legends: 0.5, 1, 2, and 5). (d) Distributions of $\Delta P_5 = P_5(\xi = 0) - P_5(\xi = -1)$ as a function of α at different values of θ_S/θ_B (indicated by legends: 0.5, 1, 2). P_{5S} indicates vertical oxygen variations associated with surface re-aeration, P_{5B} indicates vertical oxygen variations associated with sediment oxygen demand.

advection of low DO waters near the surface and upstream advection of high DO waters near the bottom. Similar to the function of P_7, P_8 has the reverse effect from that of P_5 and P_6 in controlling vertical DO stratifications.

The relative importance of P_5, P_6, P_7 and P_8 in controlling oxygen stratification in estuaries depends on the relative magnitudes of $\theta_S/\gamma H$, $\theta_B/\gamma H$, P_M/γ, $\overline{O}_x\overline{u}/\gamma$, and $\overline{O}_x u_E/\gamma$. $O(\gamma)$ is around 10^{-6} s^{-1} (Chapra, 1997; Borsuk et al., 2001). The

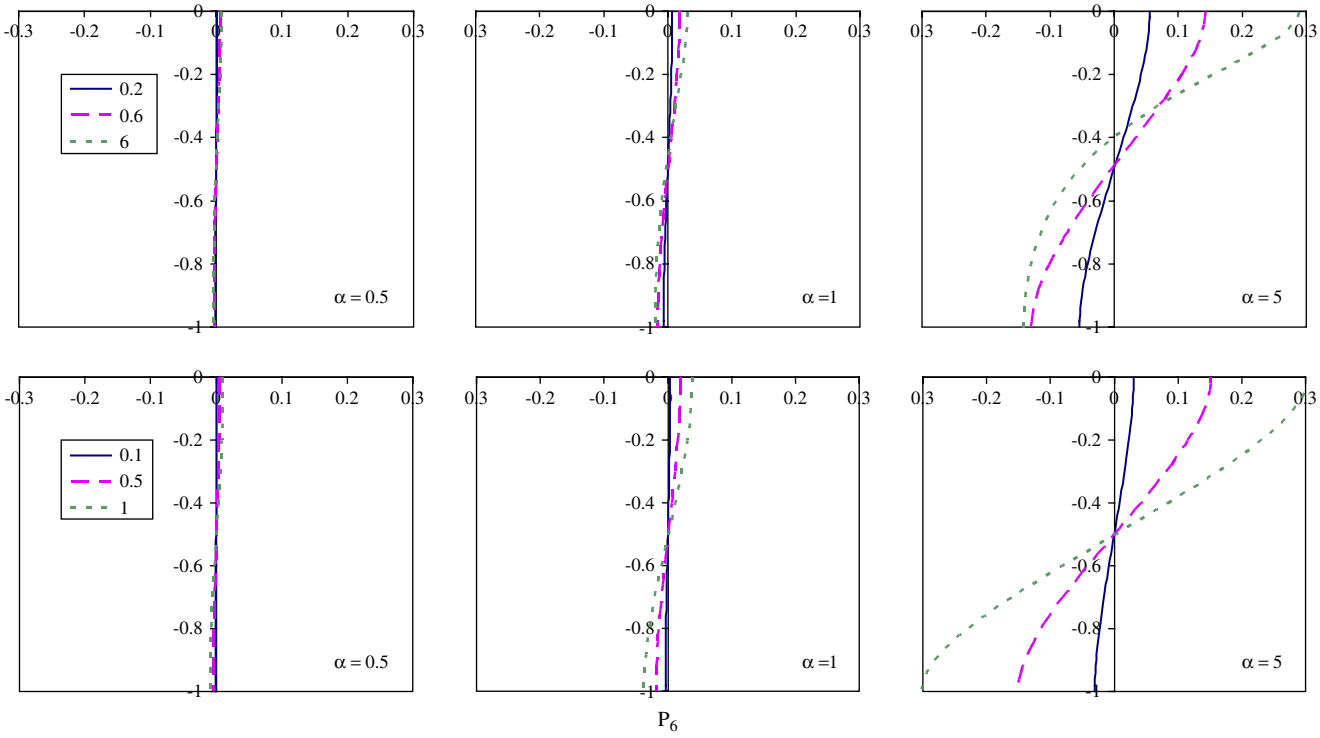

Fig. 3. Vertical distributions of P_6 at different values of α with an exponential function (upper panel) and a linear function (bottom panel) of photosynthetic oxygen production assumed. The legends in the figures indicate different values of k (constant in the exponential function, upper panel) and λ (constant in the linear function, lower panel).

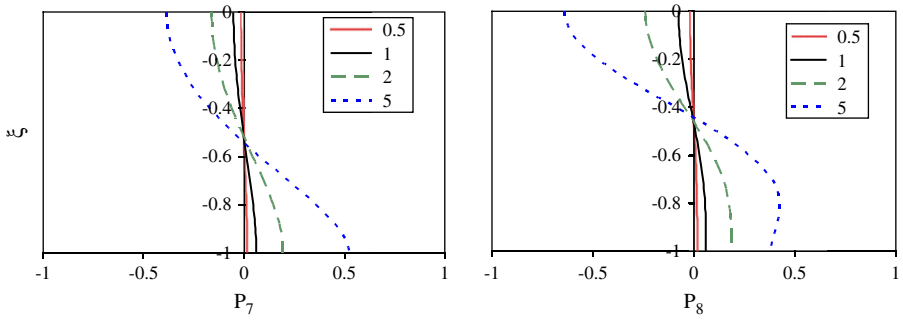

Fig. 4. Vertical distributions of P_7 (left) and P_8 (right) at different values of α. P_7 indicates vertical oxygen variations associated with the vertical sheer of the mean flow, and P_8 indicates vertical oxygen variations associated with the estuarine gravitational circulation. The legends in the figures indicate different values of α.

surface oxygen flux, $\theta_S = K_S(\partial O/\partial z)$, $z = 0$, is usually a function of wind and water velocities in estuaries, $O(\theta_S) \approx 1\ g\ m^{-2}\ day^{-1}$ (Thomann and Mueller, 1987; Chapra, 1997). Typical values of SOD for estuarine mud range between 1 and 2 $g\ m^{-2}\ day^{-1}$ (Chapra, 1997). $O(P_M)$ is generally between 0.1 and 1 $mg\ l^{-1}\ day^{-1}$ for moderately to highly productive systems (Chapra, 1997). Based on the observations in the Cape Fear and the Pamlico River Estuaries in North Carolina, $O(\overline{O}_x)$ is generally around $10^{-4}\ mg\ l^{-1}\ m^{-1}$, $O(\overline{u})$ is around $10^{-2}\ m\ s^{-1}$ and occasionally reaches $10^{-1}\ m\ s^{-1}$ during high flow events. $O(u_E)$ is between 10^{-2} and $10^{-1}\ m\ s^{-1}$ (Carpenter and Yonts, 1979; Stanley and Nixon, 1992; Mallin et al., 1999). Therefore, with a 10-m water depth, $O(\theta_S/\gamma H) \approx O(\theta_B/\gamma H) \approx 1\ mg\ l^{-1}$, $O(P_M/\gamma) \approx 1-10\ mg\ l^{-1}$, $O(\overline{O}_x\overline{u}/\gamma) \approx 1\ mg\ l^{-1}$, and $O(\overline{O}_x u_E/\gamma) \approx 1-10\ mg\ l^{-1}$. The oxygen stratification resulted from the combination of the four terms in Eq. (17), hence, exhibits vertical trends from highly stratified (with bottom hypoxia likely to occur) to well mixed (with bottom hypoxia rarely occurring) as mean flow and gravitational circulation become stronger. Kuo and Neilson (1987) attributed the rare occurrence of hypoxic conditions in the James River (compared with the York and Rappahanoke Rivers) in Virginia to a stronger gravitational circulation, which agrees well with the findings here.

Photosynthetic oxygen production, the vertical distribution of which is not available in both Pamlico and Cape Fear Rivers, is assumed to be uniformly distributed in the following discussions and case studies. In addition, the surface and bottom oxygen fluxes (θ_S and θ_B, respectively), which usually have the same order of magnitude, are assumed to be equal in the following analysis and discussions.

2.1. Estuarine gravitational circulation u_E and α

In order to investigate the impacts of u_E (the strength of the gravitational circulation) and α (relative importance between BOD consumption and vertical diffusivity) on vertical oxygen distributions in partially-mixed estuaries, oxygen stratifications at different values of u_E and α are presented in Fig. 5. Based on the observations from the US Geological Survey (USGS) and the Lower Cape Fear River Program (LCFRP: http://www.uncwil.edu/cmsr/aquaticecology/lcfrp/), typical values of the parameters are selected to represent mean flow conditions of the Cape Fear River, where $H = 10$ m, $\theta_S = \theta_B = 1 \times 10^{-5}\ g\ m^{-2}\ s^{-1}$, $\gamma = 10^{-6}\ s^{-1}$, $\overline{O}_x = 0.8 \times 10^{-4}\ mg\ l^{-1}\ m^{-1}$, and $\overline{u} = 0.01\ m\ s^{-1}$.

Vertical profiles of dissolved oxygen usually exhibit a stratification trend of higher concentrations near the surface and lower near the bottom, due to oxygen sources existing near the surface. A strong river flow and/or estuarine gravitational mode usually reduce the stratification. However, the importance of this mode in modifying the oxygen stratification is quite different in different systems. The difference in oxygen profiles between a stronger (e.g. $u_E = 10\ cm\ s^{-1}$) and a weaker (e.g. $1\ cm\ s^{-1}$) gravitational mode is negligible when α is below or around 0.5 (Fig. 5) or, when vertical diffusion is strong and/or BOD is relatively small in a system. As α increases (i.e. vertical diffusion decreases and/or BOD increases, and when the bottom-water hypoxia is more likely to occur), the impacts of gravitational circulation on vertical oxygen distribution becomes more pronounced. In some cases (e.g. $\alpha = 1-2$, $\overline{O}_x > 0$, $\theta_S = \theta_B = 10^{-5}\ g\ m^{-2}\ s^{-1}$), a strong gravitational circulation (around $10\ cm\ s^{-1}$) can even lead to lower oxygen concentrations near the surface and higher near the bottom.

As u_E increases, vertical DO stratification appears to be less sensitive to the value of α. The impact of α on oxygen stratification is profound (Fig. 6). As α increases, the four terms in Eq. (17), which determine the vertical oxygen profiles affected by surface re-aeration and SOD (P_{5S} and P_{5B}, respectively, for the case of $\theta_S = \theta_B$, $P_5 = P_{5S} + P_{5B}$), photosynthesis (P_6), river flow (P_7), and estuarine gravitational circulation (P_8), increase (Figs. 2–4). Among the four terms, P_5 and P_6 lead to higher near-surface and lower near-bottom oxygen concentrations with P_7 and P_8 contributing to an opposite trend (with the assumption of $\overline{O}_x > 0$). When α is small ($\alpha < 0.5$), vertical mixing is strong and the surface-to-bottom difference in DO (ΔDO) is negligible with the above listed parameters. As α increases ($0 < \alpha < 2$), ΔDO becomes larger under weaker gravitational circulation ($u_E \leq 5\ cm\ s^{-1}$) condition, and becomes smaller (more negative) under strong gravitational circulation condition ($u_E \geq 10\ cm\ s^{-1}$). As α continues to increase, vertical mixing is further suppressed, DO stratification is enhanced even when gravitational circulation is strong.

The variation of ΔDO under different u_E conditions suggests that P_5 and P_6 dominate the oxygen stratification with a weak to moderate gravitational circulation mode

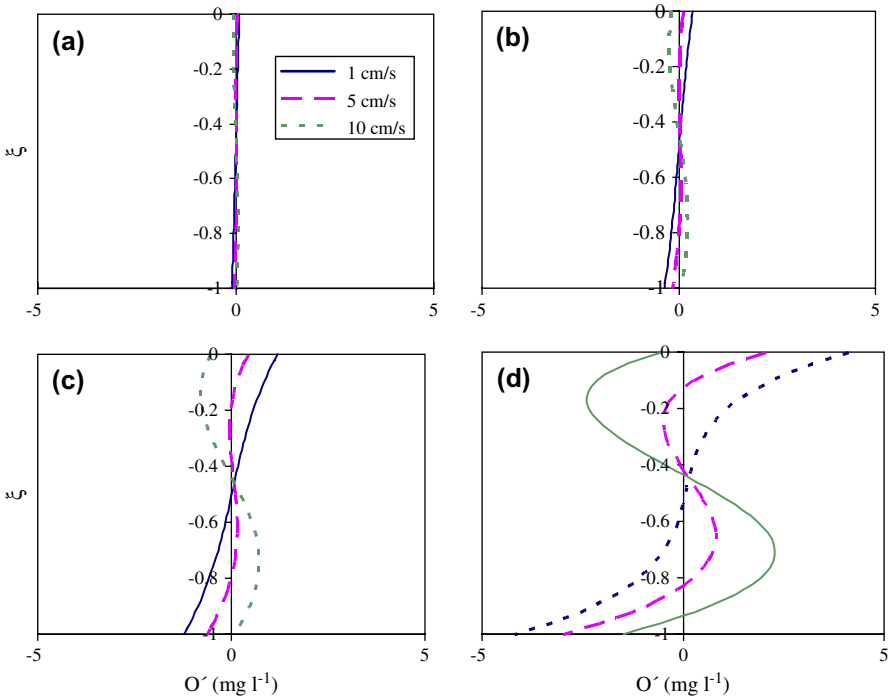

Fig. 5. Vertical distributions of O' (deviations of dissolved oxygen concentrations from depth-averaged values) at different values of u_E (indicated by legends: 1, 5, 10 cm s^{-1}) when α is (a) 0.5, (b) 1, (c) 2, and (d) 5.

($u_E \leq 5$ cm s^{-1}). As gravitational circulation being stronger ($u_E \geq 10$ cm s^{-1}), its effect on oxygen stratification is not significant when vertical mixing is weak ($\alpha > 2$) but becomes dominant with moderate to strong vertical mixing ($0 < \alpha < 2$), resulting in reversed oxygen stratification. This extreme case (reversed oxygen stratification) was observed occasionally in the Cape Fear River Estuary (Fig. 7).

The impact of estuarine gravitational circulations on DO stratification was discussed above with river flow assumed to be constant. River flow is a function of freshwater discharge, which varies with time. The impact of river flow on DO stratification follows a similar trend as that of gravitational circulation, often with a smaller magnitude.

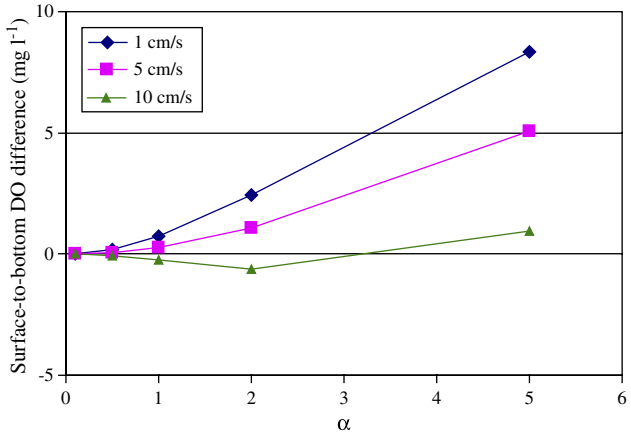

Fig. 6. The variation of surface-to-bottom differences in dissolved oxygen concentrations as a function of α at different values of u_E (indicated by legends: 1, 5, 10 cm s^{-1}).

2.2. Along-channel gradient of depth-averaged oxygen concentration

Eq. (17) also sheds light on the most vulnerable places where bottom hypoxia is likely to occur. We have assumed the longitudinal gradient of the depth-averaged oxygen concentration, $\overline{O}_x$, to be positive in the above discussions; however, in upper estuaries, $\overline{O}_x$ is often negative (Kuo et al., 1991; Buzzelli et al., 2002), due to shallower and hence more easily aerated waters in the freshwater streams and deeper, less aerated waters downstream. In such cases, the vertical oxygen profiles governed by the four functions in Eq. (17) all have a trend of higher surface and lower bottom oxygen concentrations. With the presence of a certain amount of BOD and SOD, hypoxic conditions may develop in the bottom waters.

In contrast, in lower estuaries, $\overline{O}_x$ is usually positive due to less polluted waters and hence lower biochemical oxygen demand near the mouth of the estuary. In such cases, vertical oxygen profiles governed by the last two functions (associated with river flow and estuarine circulation) in Eq. (17) have a trend of lower surface and higher bottom oxygen concentrations, which counteracts the vertical profile governed by the first two functions (associated with surface re-aeration/SOD and photosynthetic oxygen production). With large river inflow and strong gravitational circulation, hypoxic conditions are less likely to develop if provided with the same amount of BOD and SOD as in the upper estuaries. Such spatial trends

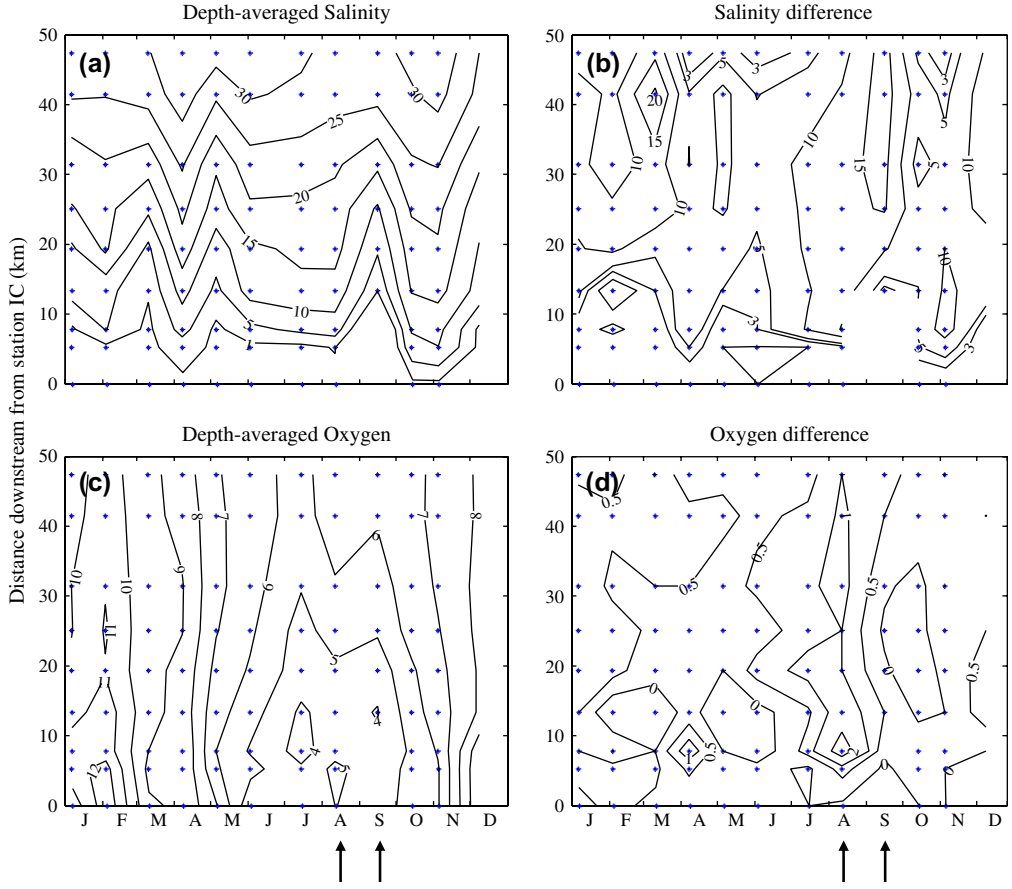

Fig. 7. Spatial and temporal distributions of (a) depth-averaged salinity, (b) surface-to-bottom difference in salinity, (c) depth-averaged DO concentration (mg l^{-1}) and (d) surface-to-bottom difference in DO concentrations in the Cape Fear River Estuary. The * indicates time and places where samples were collected, and the arrows indicate the selected cases.

in $\overline{O}_x$ can often lead to a pro-hypoxia zone in the upper portions of an estuary.

3. Cape Fear River Estuary (CFRE)

The CFRE is located in southeastern North Carolina (NC). Its principal channel is the Cape Fear River, extending to Greensboro, NC, in the Piedmont. The lower river is joined by two ''black water'' tributaries, the Black River and the Northeast Cape Fear River, originating in the coastal plain (the term ''black water'' refers to the color of the water). The CFRE is hereafter referred to as the estuarine portion of the lower Cape Fear River, which empties directly into the Atlantic Ocean.

The CFRE is narrow, ranging from 2 to 3 km in width and extends about 50 km from the general location of the salt boundary near Wilmington, NC, to the river mouth at Bald Head Island. A 12.8-m deep ship channel is maintained from Wilmington to the river entrance by the US Army Corps of Engineers. The channel is flanked with broad shallow shoals. The mean tidal range is around 1.3 m near the river mouth and 1.2 m near Wilmington. The vertical salinity difference usually ranges from 5 to 20 in the middle portions of the estuary, but tends to be better mixed toward the river mouth. The classical two-layer estuarine circulation is not dominant near the river mouth, but becomes important in the reach of the CFRE seaward of the Snows Marsh area (Carpenter and Yonts, 1979; Pietrafesa and Janowitz, 1988). The 30-year averaged freshwater discharge to the estuary is around 307 $m^3 s^{-1}$ (Carpenter and Yonts, 1979). The CFRE is a micro-tidal, partially-mixed estuary. The estuary is not constrained by barrier islands and thus the estuarine flushing time is rapid, with a median of 7 days (Ensign et al., 2004).

The total drainage area of the Cape Fear River is about 23,310 km^2, contained entirely within the state of NC. Over one-half of the land in the river basin is forested; the remainder includes cultivated crop and pastureland or is urbanized. Agricultural and urban runoff from the increasing population has introduced large quantities of inorganic nutrients and has led to considerable water quality degradation in this region. The basin is also the most heavily industrialized river basin in the state with numerous point source discharges. Industrial-scale swine production has grown rapidly in recent years (around 10 million in 1998), with over half of North Carolina's swine population concentrated in the Cape Fear River basin (Cahoon et al., 1999; Mallin, 2000). Intensive livestock operations, principally swine and poultry, also contribute to the nutrient pool emptying into the CFRE (NCDENR, 1996, 2004; Cahoon et al., 1999; Mallin et al., 1999, 2002). A detailed

description of the temporal and spatial patterns of nutrient and chlorophyll *a* concentrations in the CFRE can be found in Mallin et al. (1999). The CFRE is categorized as moderately eutrophic (Bricker et al., 1999).

Dissolved oxygen concentrations in the CFRE are usually around or a little below the NC water quality standard of 5.0 mg l^{-1} during summer. Severe hypoxia (DO < 2 mg l^{-1}) often occurs following animal waste spills and hurricanes. However, no significant difference was found between average surface and bottom DO levels (Mallin et al., 1999, 2002). Salinity and DO data collected by the Lower Cape Fear River Program (http://www.uncwil.edu/cmsr/aquaticecology/lcfrp/), together with river discharge data from USGS during 2004, are used here to further investigate the controlling mechanisms of potential DO stratification in the system.

Fig. 7 shows the spatial and temporal distributions of the depth-averaged and the surface-to-bottom difference in salinity and DO concentrations along the channel of CFRE. Since the CFRE empties directly into the Atlantic Ocean, the along-channel gradient of depth-averaged salinity is relatively high, usually around 0.75×10^{-3} m^{-1} and higher during large river discharge events. The along-channel gradient of depth-averaged oxygen concentrations is negligible year-round except during summer and winter with the onset of a positive gradient around 0.07×10^{-3} mg l^{-1} m^{-1}, and a negative gradient around -0.05×10^{-3} mg l^{-1} m^{-1}, respectively. The winter oxygen gradient is mainly caused by a difference in oxygen saturation due to lower water temperature landward and higher temperature seaward. Since biological activity is very low during winter, oxygen stratification is not a concern. During summer, the along-channel oxygen gradient together with the shear caused by freshwater inflow and the gravitational circulation will modify the vertical oxygen stratification. Salinity stratification is the strongest in the middle portions of the CFRE, with the surface-to-bottom difference in salinity ranging from 10 to 20 during 2004.

Although strong salinity stratification exists in the CFRE, only moderate oxygen stratification is developed occasionally. Survey data during August and September 2004 are selected to represent the cases of moderate oxygen stratification and no oxygen stratification, respectively, to further explore the mechanisms controlling oxygen distributions in the system.

During August 10, 2004, the daily mean freshwater discharge was very low, around 80.7 m^3 s^{-1}, which set a salinity gradient of around 0.71×10^{-3} m^{-1}. The along-channel oxygen gradient was negative near the head of salt intrusion, and became positive in the downstream portions of the CFRE. As a result, a local maximum oxygen stratification was obtained where $\overline{O}_x$ was negative (and the P_5, P_7 and P_8 all work toward higher oxygen concentration near surface and lower near bottom), the stratification weakened in the downstream direction where $\overline{O}_x$ became positive. A weak oxygen stratification was still maintained in the downstream portions of the CFRE since the functions of P_7 resulting from very low freshwater inflow and P_8 resulting from the gravitational circulation do not completely offset the oxygen difference set by function P_5. If we then apply Eq. (17) with the parameters derived from the field data (Table 1), we see that the predicted oxygen stratification by Eq. (17) agree well with the observations (Fig. 8).

During September 14, 2004, the freshwater discharge was about 560.2 m^3 s^{-1}, which was much larger than that of August 10. The high salinity water was pushed further downstream and a stronger longitudinal salinity gradient formed (Fig. 7a, Table 1). As a result, both freshwater inflow and the two-layer estuarine circulation became stronger, and consequently offset the oxygen stratification effected by surface re-aeration and SOD. Dissolved oxygen was well mixed in the water column (Fig. 8b).

4. Pamlico River Estuary (PRE)

The PRE is herein referred to as the estuarine portion of the Tar–Pamlico River. The Tar–Pamlico River is one of the major tributaries in the Albemarle–Pamlico Sound Estuary System (APES) (Fig. 1). The Tar–Pamlico River has a total

Table 1
Parameters used in oxygen stratification prediction

Study sites	Cape Fear River Estuary		Pamlico River Estuary	
Measurement dates	08/10/2004	09/14/2004	09/01/2003	09/12/2003
$\overline{s}_x$ (10^{-3} m^{-1})	0.71	0.92	−0.03	0.06
$\overline{O}_x$ (10^{-3} mg l^{-1} m^{-1})	−0.023[b]/0.067[c]	0.077	0.11	0.09
$\overline{u}$ (10^{-2} m s^{-1})	1.8	12	0.28	0.32
u_E (10^{-2} m s^{-1})	11	15	−0.3	0.06
Mean tidal range (m)	1.1[a]	1.4[a]	0.15–0.3	0.15–0.3
γ (10^{-6} s^{-1})	1	1	1	1
α	1	1	2	0.5
θ_S, θ_B (10^{-5} g m^{-2} s^{-1})	2.5	2.5	1.25	1
$\frac{\theta_S}{\gamma H}$, $\frac{\theta_B}{\gamma H}$ (mg l^{-1})	2.5	2.5	2.5	2
$\frac{\overline{O}_x \overline{u}}{\gamma}$ (mg l^{-1})	−0.414[b]/1.206[c]	9.24	0.308	0.288
$\frac{\overline{O}_x u_E}{\gamma}$ (mg l^{-1})	−2.53[b]/7.37[c]	11.55	−0.33	0.054

[a] Daily mean near Wilmington.
[b] Upstream.
[c] Downstream.

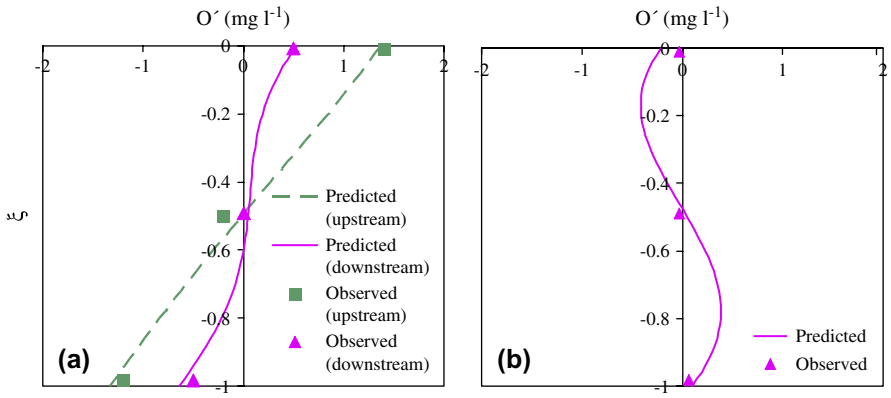

Fig. 8. The predicted (lines) depth-varying DO profile overlaid with the observed data on (a) 8/10/2004 at stations HB (upstream) and M42 (downstream), and (b) 9/14/2004 at station M42 in the Cape Fear River Estuary.

basin area of about 14,000 km^2, and is contained entirely within the State of North Carolina. The freshwater portion of the Tar–Pamlico River is usually referred to as the Tar River. Rising in the Piedmont farmlands, the Tar River flows southeasterly for 225 km. As the river flows across the flat Coastal Plain, it transforms from a freshwater river into a brackish system near the city of Washington. Here the name changes to the Pamlico River, and it travels another 60 km before emptying into the Pamlico Sound.

The long-term average freshwater input to the Pamlico River is about 150 $m^3 s^{-1}$, which contributes to a horizontal salinity distribution of near zero at the head of the estuary and about 25 at the mouth. The PRE is a shallow estuary with a mean depth of 2.7 m and channel depths ranging from around 5 m near the mouth to around 3 m near the head of the estuary. Strong stratification sometimes occurs in the middle estuary with top-to-bottom differences in salinity reaching about 8. Mixing events can occur very rapidly (within less than an hour) (Bales and Robbins, 1995). Lunar tides in the PRE are negligible. The averaged tidal range is about 0.3 m at the head of the PRE and about 0.15 m at the mouth (Stanley and Nixon, 1992; Bales and Robbins, 1995). The circulation in the Lower Tar–Pamlico River is dominated by wind- and density-driven currents (Pietrafesa et al., 1986; Phillips, 1989). The PRE is classified as a micro-tidal, partially-mixed estuary. Tidal flushing is constrained by barrier islands (the Outer Banks) enclosing Pamlico Sounds.

As a result of large amounts of nutrient loading from its drainage basins and low flushing rate (Pietrafesa et al., 1986; Pietrafesa and Janowitz, 1991; Stanley, 1993), the Tar–Pamlico River has exhibited various ecological problems such as eutrophication, hypoxia, harmful algal blooms, massive fish kills, and declining shell fish production (Pietrafesa and Miller, 1997; Mallin et al., 2000) and was categorized as highly eutrophic (Bricker et al., 1999).

Hypoxia in the PRE was first documented in the late 1960s (Hobbie et al., 1975), and was investigated more thoroughly in the mid-1970s (Davis et al., 1978). Most recently, Stanley and Nixon (1992) examined a 15-year set of biweekly measurements along the channel of the PRE, and found that hypoxia occurs most often in summer when high water temperature decreases oxygen saturation and enhances biological oxygen demand. In July, 75% of the DO readings were less than 5 $mg l^{-1}$ and more than 30% were less than 1 $mg l^{-1}$. Severe hypoxia occurs more frequently in the upper half of the estuary than near the mouth. In contrast to the CFRE, vertical DO stratification and salinity stratification are tightly coupled with variations in freshwater discharge and wind stress.

Three months (July–September 2003) of surface and bottom daily averaged salinity and DO concentrations at two stations in the middle portions of the PRE were obtained from USGS (http://waterdata.usgs.gov/nwis). The data were examined together with the river discharge (from USGS), and wind (from National Climate Data Center (NCDC) of National Oceanic and Atmospheric Administration (NOAA)) data to further explore the mechanisms controlling oxygen stratification in the PRE. Fig. 9 shows temporal variations of river flow, wind, salinity, longitudinal salinity gradient, DO, and longitudinal DO gradient at USGS station 0208453300. The depth-averaged salinity/DO is estimated as the mean of the surface and bottom concentrations, and the longitudinal gradient is obtained as the difference between the depth-averaged concentrations at stations 0208453300 and 0208455155 divided by the distance between the two stations.

In the middle of August, a large river discharge pushed freshwater downstream, as a result, both surface and bottom salinity at station 0208453300 became zero (Fig. 9). The longitudinal salinity gradient increased from 0.07×10^{-3} m^{-1} on August 7 to 0.17×10^{-3} m^{-1} on August 17, indicating a stronger estuarine gravitational circulation being formed. Consequently, salinity stratification became stronger toward the end of August. At the same time, the longitudinal salinity gradient decreased as river discharge decreased. Although the longitudinal salinity gradient fell below zero in the beginning of September, indicating a much weakened or reversed estuarine circulation in the region, strong salinity stratification persisted until September 8. The destruction of the salinity stratification lasted a couple of days after September 8, probably caused by strong vertical mixing due to increased wind speeds. The surface-to-bottom differences in DO

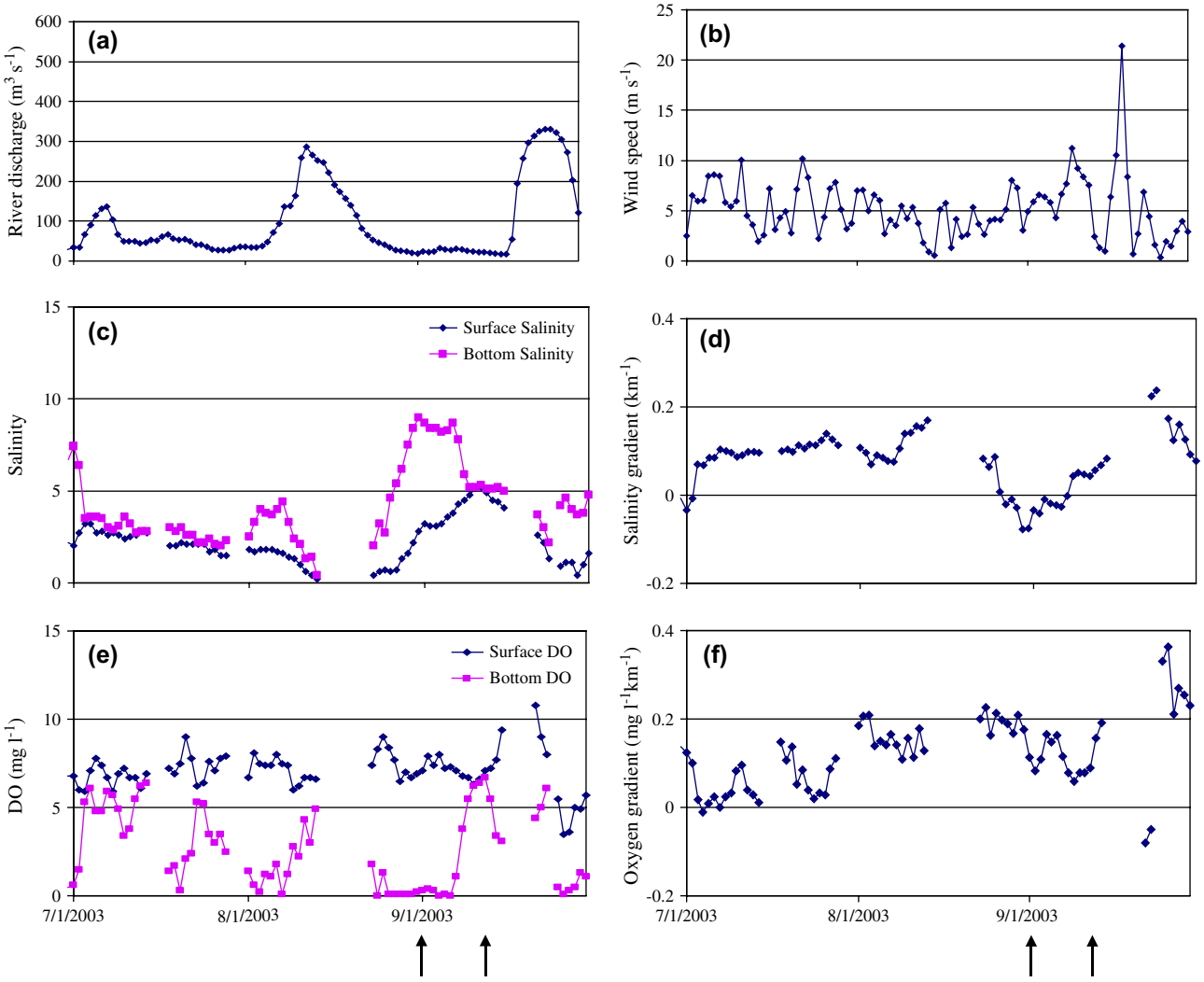

Fig. 9. The temporal variation of (a) river discharge, (b) wind speed, (c) surface and bottom salinities, (d) longitudinal salinity gradient, (e) surface and bottom DO concentrations, and (f) longitudinal DO gradient during 7/1/2003–9/30/2003 at USGS station 0208453300 in the Pamlico River Estuary.

concentrations followed closely those in salinity. With strong salinity stratification, bottom DO reached near zero. In contrast, as salinity stratification disappeared, DO concentrations became well mixed in the water column. The coincidence of vertical salinity and DO stratification indicates that the strength of vertical mixing is perhaps the most dominant factor controlling vertical DO distributions during the summertime in the PRE. Strong salinity and DO stratification often occur following large river discharge, and persist until a strong vertical mixing event breaks the stratification. In this system, estuarine gravitational circulation has little direct influence in modifying the vertical distributions of DO. The impact of both estuarine gravitational circulation mode and river discharge on DO stratification is through their roles in regulating salinity stratification and hence the intensity of vertical mixing.

Two cases (September 1 and 12, 2003) were selected to further investigate the impact of vertical mixing, estuarine circulation, and river flow on vertical DO stratification. The vertical distributions of DO derived from Eq. (17) are presented in Fig. 10. Strong vertical oxygen stratification existed on September 1 and weak stratification occurred on September 12. The parameters used in the prediction are listed in Table 1 for comparison. The longitudinal salinity and oxygen gradient ($\overline{s}_x$ and $\overline{O}_x$), $\overline{u}$ and u_E were calculated from the data. The values of α and θ_S/θ_B were estimated from general information (e.g. river depth, system classification, mean tidal range, and wind speed) and prediction calibration. During September 1 and 12, although longitudinal oxygen gradients were relatively high (compared to CFRE), both $\overline{u}$ and u_E were very low, and hence they had little impact on oxygen stratification.

The differences in oxygen stratification between the two cases were mainly caused by higher values of α during September 1 and lower values during September 12. A higher value of α can result from a larger BOD and/or weaker vertical mixing. The mid-August high river discharge event probably introduced a large amount of organic matter, which led to a bigger BOD pool in the system. Tides are negligible in the PRE. The major sources of vertical mixing are from wind and river-induced estuarine circulation, and neither was strong

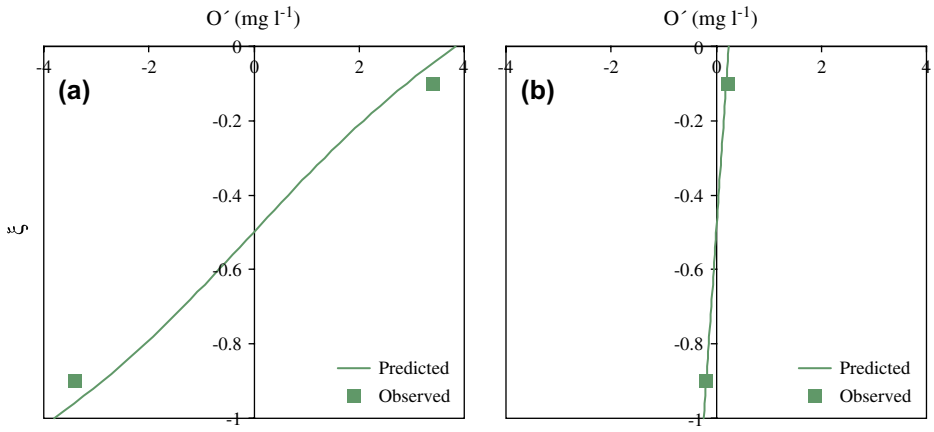

Fig. 10. The predicted depth-varying DO profile overlaid with the observed data on (a) 9/1/2003 and (b) 9/12/2003 at USGS station 0208453300 in the Pamlico River Estuary.

on September 1, leading to a higher value of α ($\alpha = 2$). In contrast, a stronger wind increased vertical mixing throughout the water column (less than 5 m deep) during September 12, leading to a lower value of α ($\alpha = 0.5$).

5. Discussion and conclusion

The most important development of this paper is the derivation of vertical oxygen stratification profile as a function of surface re-aeration and SOD (P_{5S} and P_{5B}, respectively, in Eq. (17), and the summation is referred to as P_5), photosynthesis (P_6), river flow (P_7), and estuarine gravitational circulation (P_8) in micro-tidal, partially-mixed estuaries. Since external sources of DO are mainly in the surface waters (i.e. surface re-aeration and photosynthesis), vertical mixing sets a DO profile of higher concentration near the surface and lower near the bottom. With an increased downstream depth-averaged DO concentration, strong river flow and gravitational circulation can both lead to lower DO concentrations near the surface and higher concentrations near the bottom.

The actual vertical oxygen profile is determined by the relative importance of the four functions, and is sensitive to values of u_E and α. Function u_E indicates the strength of the classical two-layer estuarine circulation, which is a function of the longitudinal salinity gradient. Vertical DO stratification usually becomes weaker as u_E increases. Such phenomena were observed in several estuaries including James River (Kuo and Neilson, 1987), Tone River (Ishikawa et al., 2004), Paerl River (Yin et al., 2004), and Cape Fear River (this paper). The impact of river flow ($\overline{u}$) on DO stratification follows the same trend as that of u_E, often with a smaller magnitude.

The importance of u_E (and $\overline{u}$) in regulating DO stratification also depends on α, which represents the relative importance of BOD and vertical mixing intensities. As α increases (i.e. vertical diffusion decreases and/or BOD increases), the impact of estuarine gravitational circulation mode on vertical oxygen distribution becomes more important.

The impact of α on oxygen stratification is profound. As u_E (and $\overline{u}$) increases, DO stratification appears to be less sensitive to the value of α. Surface-to-bottom differences in DO concentrations are negligible when α is small ($\alpha < 0.5$). As α increases, ΔDO increases under a weak to moderate gravitational circulation mode ($u_E \leq 5\ \mathrm{cm\ s^{-1}}$). Under a strong gravitational circulation mode, ΔDO becomes negative with a small α ($\alpha < 2$), and as α continues to increase, ΔDO becomes positive. The turning point indicates a P_8 (and P_7) dominant oxygen profile when α is small and a P_5 (and P_6) dominant oxygen profile when α is large.

Implementation of the governing equation for vertical oxygen stratification (Eq. (17)) was conducted on two micro-tidal, partially-mixed estuarine systems: the Cape Fear River Estuary and the Pamlico River Estuary. In the Cape Fear River, de-coupling between vertical salinity stratification and oxygen stratification is mainly due to a relatively stronger gravitational circulation mode and higher freshwater inflow, which tend to introduce lower oxygen waters near the surface and higher oxygen waters near the bottom. This counteracts the vertical oxygen profile set up by surface re-aeration and SOD. With stronger river flow and estuarine gravitational circulation, DO stratification is less sensitive to the value of α. Therefore, even with a strong salinity stratification (a large α value), DO concentrations tend to be well mixed in the water column.

In contrast to the CFRE, in the Pamlico River Estuary, with negligible influence from tidal mixing, the system is sensitive to vertical mixing regulated by salinity stratification and wind. Estuarine gravitational circulation and river flow are usually weak, and hence DO stratification (compared with that in CFRE) is more sensitive to the value of α. In the PRE, with large quantities of organic matter input and high phytoplankton production rate, oxygen consumption by BOD is relatively fast, and hence the value of α is very sensitive to the effects of vertical diffusion. Therefore, a strong correlation usually develops between vertical stratification in salinity and DO. Examples of such cases also include Neuse River (Borsuk et al., 2001; Buzzelli et al., 2002), Swan River (Kurup and Hamilton, 2002), and Patuxent River (Breitburg et al., 2003).

In the theoretical derivations of this study, vertical diffusivity is assumed to be constant. In reality, it may vary as

a function of mixing length, velocity shear, and vertical density stratification. Variations of the vertical diffusivity in a water column may result in a different shape of the vertical oxygen profile, but the general trends of the impacts of surface re-aeration/SOD, photosynthesis, river flow, and estuarine gravitational circulation on oxygen stratification may remain. Wind is considered here as a source of vertical mixing, so the impact of wind-induced circulation on oxygen dynamics is deemed beyond the scope of this paper.

Acknowledgement

The authors would like to thank the two anonymous reviewers for their careful review and valuable suggestions. We appreciate very much the suggestions provided by Albert Y. Kuo. This study is partly supported by the Coastal Ocean Research and Monitoring Program (CORMP) under NOAA Grand #NA16RP2675 via the National Ocean Service, through Charleston Coastal Services Center. CORMP is a partnership between the University of North Carolina at Wilmington and North Carolina State University.

References

Bales, J.D., Robbins, J.C., 1995. Simulation of hydrodynamics and solute transport in the Pamlico River Estuary, North Carolina. U.S. Geological Survey Open-File Report 94-454, 85 pp.

Bergondo, D.L., Kester, D.R., Stoffel, H.E., Woods, W.L., 2005. Time-series observations during the low sub-surface oxygen events in Narragansett Bay during summer 2001. Marine Chemistry 97 (1/2), 90–103.

Boesch, D.F., 2002. Challenges and opportunities for science in reducing nutrient over-enrichment of coastal ecosystems. Estuaries 25, 744–758.

Borsuk, M.E., Stow, C.A., Luettich Jr., R.A., Paerl, H.W., Pinckney, J.L., 2001. Modelling oxygen dynamics in an intermittently stratified estuary: estimation of process rates using field data. Estuarine, Coastal and Shelf Science 52, 33–49.

Breitburg, D.L., Adamack, A., Rose, K.A., Kolesar, S.E., Decker, M.B., Purcell, J.E., Keister, J.E., Cowan Jr., J.H., 2003. The pattern and influence of low dissolved oxygen in the Patuxent River, a seasonal hypoxic estuary. Estuaries 26 (2A), 280–297.

Bricker, S.B., Clement, C.G., Pirhalla, D.E., Orlando, S.P., Farrow, D.R.G., 1999. National Estuarine Eutrophication Assessment: Effects of Nutrient Enrichment in the Nation's Estuaries. Special Projects Office and National Centers for Coastal Ocean Science, National Ocean Service, National Oceanic and Atmospheric Administration, Silver Spring, MD, 71 pp.

Buzzelli, C.P., Luettich Jr., R.A., Powers, S.P., Peterson, C.H., McNinch, J.E., Pinckney, J.L., Paerl, H.W., 2002. Estimating the spatial extent of bottom-water hypoxia and habitat degradation in a shallow estuary. Marine Ecology Progress Series 230, 103–112.

Cahoon, L.B., Mikucki, J.A., Mallin, M.A., 1999. Nitrogen and phosphorous imports to the Cape Fear and Neuse River Basins to support intensive livestock production. Environmental Science and Technology 33, 410–415.

Carpenter, J.H., Yonts, W.L., 1979. Dye tracer and current meter studies: Cape Fear estuary, 1976, 1977 & 1978. Carolina Power & Light, Southport, North Carolina.

Cerco, C.F., Cole, T., 1993. Three-dimensional eutrophication model of Chesapeake Bay. Journal of Environmental Engineering 119, 1006–1025.

Chapra, S.C., 1997. Surface Water-quality Modeling. WCB McGraw-Hill, 844 pp.

Cloern, J.E., 2001. Our evolving conceptual model of the coastal eutrophication problem. Marine Ecology Progress Series 210, 223–253.

Davis, G.J., Brinson, M.M., Burke, W.A., 1978. Organic Carbon and Deoxygenation in the Pamlico River Estuary (Report No. 131). University of North Carolina, Water Resources Research Institute, Raleigh, North Carolina, 123 pp.

Diaz, R.J., Rosenberg, R., 1995. Marine benthic hypoxia: a review of its ecological effects and the behavioral responses of benthic macrofauna. Oceanography and Marine and Biology: An Annual Review 33, 245–303.

Diaz, R.J., Nestlerode, J., Diaz, M.L., 2004. A global perspective on the effects of eutrophication and hypoxia on aquatic biota. In: Rupp, G.L., White, M.D. (Eds.), Proceedings of the Seventh International Symposium on Fish Physiology, Toxicology, and Water Quality, Tallinn, Estonia, May 12–15, 2003. U.S. Environmental Protection Agency, Ecosystem Research Division, Athens, Georgia, USA, pp. 1–33. EPA 600/R-04/049.

Dyer, K.R., 1997. Estuaries: A Physical Introduction. John Wiley and Sons, Chichester, England.

Eby, L.A., Crowder, L.B., 2002. Hypoxia-based habitat compression in the Neuse River Estuary: context-dependent shifts in behavioral avoidance thresholds. Canadian Journal of Fisheries and Aquatic Sciences 59 (6), 952–965.

Eby, L.A., Crowder, L.B., 2004. Effects of localized hypoxic disturbances on an estuarine fish and crustacean community: a multi-scale approach. Estuaries 27 (2), 342–351.

Ensign, S.H., Halls, J.N., Mallin, M.A., 2004. Application of digital bathymetry data in an analysis of flushing times of two large estuaries. Computers & Geosciences 30, 501–511.

Glenn, S., Arnone, R., Bergmann, T., Bissett, W.P., Crowley, M., Cullen, J., Gryzmski, J., Haidvogel, D., Kohut, J., Moline, M., Oliver, M., Orrico, C., Sherrell, R., Song, T., Weidemann, A., Chant, R., Schofield, O., 2004. Biogeochemical impact of summertime coastal upwelling on the New Jersey Shelf. Journal of Geophysical Research 109 (C12S02), doi:10.1029/2003JC002265.

Hagy, J.D., Boynton, W.R., Keefe, C.W., Wood, K.V., 2004. Hypoxia in Chesapeake Bay, 1950–2001: long-term change in relation to nutrient loading and river flow source. Estuaries 27 (4), 634–658.

Hansen, D.V., Rattray Jr., M., 1965. Gravitational circulation in straits and estuaries. Journal of Marine Research 23, 104–122.

Hetland, R.D., Geyer, W.R., 2004. An idealized study of the structure of long, partially mixed estuaries. Journal of Physical Oceanography 34, 2677–2691.

Hobbie, J.E., Copeland, B.J., Harrison, W.G., 1975. Sources and fates of nutrients in the Pamlico River Estuary, North Carolina. In: Cronin, L.E. (Ed.), Chemistry, Biology, and the Estuarine System. Estuarine Research, vol. I. Academic Press, New York, pp. 287–302.

Holmer, M., 1999. The effect of oxygen depletion on anaerobic organic matter degradation in marine sediments. Estuarine, Coastal and Shelf Science 48, 383–390.

Howarth, R.W., Marino, R., Scavia, D., 2003. Nutrient Pollution in Coastal Waters: Priority Topics for an Integrated National Research Program for the United States. U.S. Department of Commerce, National Oceanic and Atmospheric Administration, Silver Spring, MD, 21 pp.

Ishikawa, T., Suzuki, T., Qian, X., 2004. Hydraulic study of the onset of hypoxia in the Tone River Estuary. Journal of Environmental Engineering 130 (5), 551–561.

Kauppila, P., Meeuwig, J.J., Pitkänen, H., 2003. Predicting oxygen in small estuaries of the Baltic Sea: a comparative approach. Estuarine, Coastal and Shelf Science 57, 1115–1126.

Kirk, J.T., 1994. Light and Photosynthesis in Aquatic Ecosystems. Cambridge University Press, Cambridge, Great Britain.

Kuo, A.Y., Neilson, B.J., 1987. Hypoxia and salinity in Virginia estuaries. Estuaries 10, 277–283.

Kuo, A.Y., Park, K., Moustafa, M.Z., 1991. Spatial and temporal variabilities of hypoxia in the Rappahannock River, Virginia. Estuaries 14 (2), 113–121.

Kurup, R., Hamilton, D.P., 2002. Flushing of dense, hypoxic water from a cavity of the Swan River Estuary, Western Australia. Estuaries 25 (5), 908–915.

Lung, W.-S., Bai, S., 2003. A water quality model for the Patuxent Estuary: current conditions and predictions under changing land-use scenarios. Estuaries 26 (2A), 267–279.

MacCready, P., 2004. Toward a unified theory of tidally-averaged estuarine salinity structure. Estuaries 27 (4), 561–570.

Mallin, M.A., Cahoon, L.B., McIver, M.R., Parsons, D.C., Shank, G.C., 1999. Alteration of factors limiting phytoplankton production in the Cape Fear River Estuary. Estuaries 22 (4), 825–836.

Mallin, M.A., 2000. Impacts of industrial-scale swine and poultry production on rivers and estuaries. American Scientist 88, 26–37.

Mallin, M.A., Burkholder, J.M., Cahoon, L.B., Posey, M.H., 2000. North and South Carolina coasts. Marine Pollution Bulletin 41 (1–6), 56–75.

Mallin, M.A., Posey, M.H., McIver, M.R., Parsons, D.C., Ensign, S.H., Alphin, T.D., 2002. Impacts and recovery from multiple hurricanes in a Piedmont-coastal plain river system. BioScience 52 (11), 999–1010.

North Carolina Department of Environment and Natural Resources (NCDENR), 1996. Cape Fear River Basinwide Water Quality Management Plan. NCDENR, Division of Water Quality, Raleigh, NC.

NCDENR, 2004. Basinwide Assessment Report, Cape Fear River Basin. NCDENR, Division of Water Quality, Environmental Sciences Section, Raleigh, NC.

Nestlerode, J.A., Diaz, R.J., 1998. Effects of periodic environmental hypoxia on predation of a tethered Polychaete, *Glycera americana*: implications for trophic dynamics. Marine Ecology Progress Series 172, 185–195.

Officer, C.B., 1976. Physical Oceanography of Estuaries (and Associated Coastal Waters). Wiley, New York.

Park, K., Kuo, A.Y., Neilson, B.J., 1996. A numerical model study of hypoxia in the tidal Rappahannock River of Chesapeake Bay. Estuarine, Coastal and Shelf Science 42, 563–581.

Peterson, C.H., Summerson, H.C., Thomson, E., Lenihan, H.S., Grabowski, J., Manning, L., Micheli, F., Johnson, G., 2000. Synthesis of linkages between benthic and fish communities as a key to protecting essential fish habitat. Bulletin of Marine Science 66 (3), 759–774.

Phillips, J.D., 1989. River discharge and sediment deposition in the Upper Pamlico Estuary. In: Neilson, B.J., et al. (Eds.), Estuarine Circulation. Humana Press, Clifton, New Jersey, pp. 337–349.

Pietrafesa, L.J., Janowitz, G.S., Chao, T.-Y., Weisberg, R.H., Askari, F., Nobel, E., 1986. The Physical Oceanography of Pamlico Sound, UNC Sea Grant Publication (UNC-SG-WP-86-5), 126 pp.

Pietrafesa, L.J., Janowitz, G.S., 1988. Physical oceanographic processes affecting larval transport around and through North Carolina inlets. American Fisheries Society Symposium 3, 34–50.

Pietrafesa, L.J., Janowitz, G.S., 1991. The Albemarle–Pamlico Coupling Study. Final Report to the Environmental Protection Agency, Washington, DC, 70 pp.

Pietrafesa, L.J., Miller, J.M., 1997. A Comparison of Fish Kills in the Pamlico and Neuse Rivers (a Symptom) and Implications for Estuarine Health. Special Report. North Carolina State University, Raleigh, NC.

Pritchard, D.W., 1952. Salinity distribution and circulation in the Chesapeake Bay estuarine system. Journal of Marine Research 11, 106–123.

Pritchard, D.W., 1954. A study of the salt balance in a coastal plain estuary. Journal of Marine Research 15, 33–42.

Scavia, D., Justiä, D., Bierman Jr., V.J., 2004. Reducing hypoxia in the Gulf of Mexico: advice from three models. Estuaries 27 (3), 419–425.

Stanley, D.W., Nixon, S.W., 1992. Stratification and bottom-water hypoxia in the Pamlico River Estuary. Estuaries 15 (3), 270–281.

Stanley, D.W., 1993. Long-term trends in Pamlico River estuary nutrients, chlorophyll, dissolved oxygen, and watershed nutrient production. Water Resources Research 29 (8), 2651–2662.

Tankersley, R.A., Wieber, M.G., 2000. Physiological responses of postlarval and juvenile blue crabs *Callinectes sapidus* to hypoxia and anoxia. Marine Ecology Progress Series 194, 179–191.

Taylor, D.L., Eggleston, D.B., 2000. Effects of hypoxia on an estuarine predator–prey interaction: foraging behaviour and mutual interference in the blue crab *Callinectes sapidus* and the infaunal clam prey *Mya arenaria*. Marine Ecology Progress Series 196, 221–237.

Thomann, R.V., Mueller, J.A., 1987. Principles of Surface Water Quality Modeling and Control. Harpers & Row, Publishers Inc., New York, 644 pp.

Wool, T.A., Davie, S.R., Rodriguez, H.N., 2003. Development of three-dimensional hydrodynamic and water quality models to support total maximum daily load decision process for the Neuse River Estuary, North Carolina. Journal of Water Resources Planning and Management 129 (4), 295–306.

Yin, K., Lin, Z., Ke, Z., 2004. Temporal and spatial distribution of dissolved oxygen in the Pearl River Estuary and adjacent coastal waters. Continental Shelf Research 24 (16), 1935–1948.

Zheng, L., Chen, C., Zhang, F.Y., 2004. Development of water quality model in the Satilla River Estuary, Georgia. Ecological Modeling 178, 457–482.